ORGANOMETALLICS

pubs.acs.org/Organometallics Article

Synthesis and Reactivity of Iron and Cobalt Bis(amidophosphine selenide) Complexes

Daniel Y. Zhou, Kelsey S. Zimmerman, Paige M. Gannon, Sebastian M. Krajewski, Werner Kaminsky, Benjamin S. Mitchell,* and Alexandra Velian*

Cite This: *Organometallics* 2025, 44, 335−339 Read Online

ACCESS | Metrics & More | Article Recommendations | Supporting Information

ABSTRACT: We report the synthesis of two metal bis(amidophosphine selenide) complexes, ML_2 (M = Fe, Co; L = $SePPh_2N^{(-)}Tol$), and investigate their reactivity toward ligand binding and oxidation with oxygen atom transfer reagents, pyridine-*N*-oxide and mesityl nitrile oxide. The oxidative strength of the reagent dictates the nature of the reactivity: either the ligand is oxidized, leading to the formation of a bimetallic mixed-ligand complex $[MLL']_n$, (L′ = $OPPh_2N^{(-)}Tol$), or the metal center is oxidized, resulting in a bimetallic μ-oxo complex $[FeL_2]_2(\mu_2\text{-O})$. This study defines a chemical space in which amidophosphine selenide ligands maintain their structural integrity.

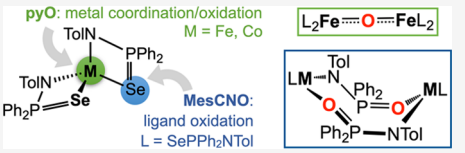

INTRODUCTION

Metal complexes featuring amidophosphine selenide ligands have been previously studied for their potential as single source precursors for the deposition of metal chalcogenide phases (M′ = Ti−Ni, Zn, and Cd)[1−4] but also as catalysts for the hydroamination of alkenes (M′ = Ln)[5] and heterocumulenes (M′ = Ti),[6,7] or in ring-opening polymerizations (M′ = Mg−Sr).[8,9] The hard amides and soft selenium atoms create a versatile coordination environment for a wide range of metals, and the metal−selenium interactions are poised to provide structural flexibility and even open coordination sites on demand.[10] At the same time, the P═Se moiety is liable to undergo chemical transformations that compromise the ligand integrity.[11−13] Here, we report the synthesis of two metal bis(amidophosphine selenide) complexes, ML_2 (M = Fe, Co; L = $SePPh_2N^{(-)}Tol$), and explore their reactivity toward ligand binding and chemical oxidation with oxygen atom transfer reagents.

Our group has employed amidophosphine ligands to anchor catalytically active "edge" sites on the surface of a cobalt selenide cluster "support" (Co_6Se_8; Figure 1).[14−17] This edge/support cluster construct provided molecular insights into metal−support interactions,[14] allosteric effects,[18] and multi-active site dynamics[17] that are at play in heterogeneous catalytic interfaces. Mapping the reactivity of the monometallic ML_2 complexes, which have identical first coordination environments to the cluster edge sites, sets the foundation for elucidating the role of the Co_6Se_8 "support" in modulating reactivity.

RESULTS AND DISCUSSION

Synthesis and Properties of ML_2. The FeL_2 and CoL_2 complexes are obtained in good yields by treating the aminophosphine selenide (L^H = $SePPh_2NHTol$) with iron or cobalt hexamethyldisilazide (Scheme 1).[1−4] Single-crystal X-ray diffraction analysis revealed that the iron and cobalt complexes are isostructural. The metal center adopts a pseudotetrahedral geometry, with two amidophosphine selenide ligands bound κ^2 through Se and N (Figure 2).[1−4] A bonding metric comparison between ML_2 complexes and the cluster edge sites they emulate reveals notable differences (Table S1). The Co_6Se_8 cluster surface constrains the Se−M−Se angles to be more acute than those in the ML_2 complexes, widening the corresponding N−M−N angles and accentuating the deviation from a tetrahedral coordination environment at

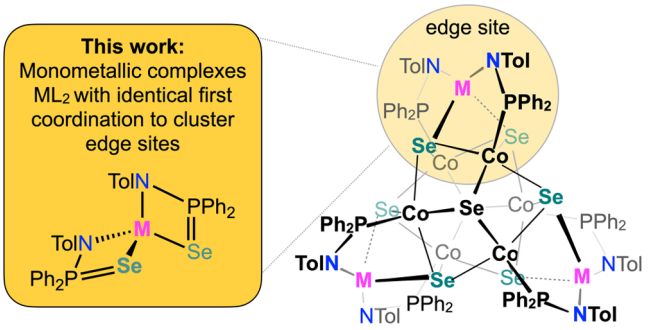

Figure 1. Monometallic amidophosphine selenide complexes ML_2 replicate the first sphere coordination environment of M/Co/Se clusters studied by our group.

Received: November 7, 2024
Revised: December 9, 2024
Accepted: December 11, 2024
Published: December 19, 2024

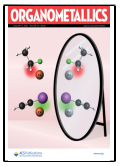

https://doi.org/10.1021/acs.organomet.4c00468
Organometallics 2025, 44, 335−339

Scheme 1. Synthesis of ML_2 Complexes (M = Fe, Co)

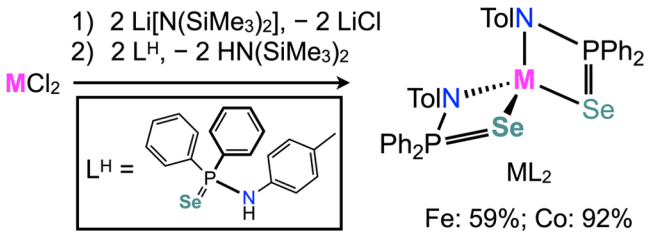

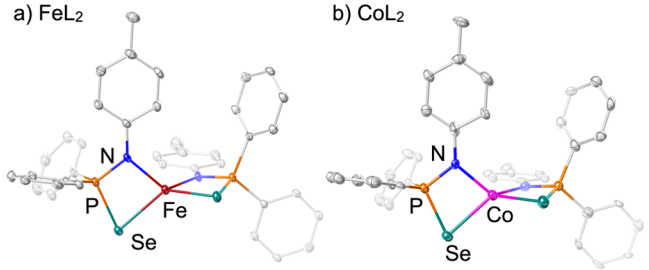

Figure 2. Solid-state structures of (a) FeL_2 and (b) CoL_2. Ellipsoids were plotted at 50% probability. Hydrogen atoms and cocrystallized solvent molecules are omitted for clarity.

the metal. For instance, Se−M−Se and N−M−N angles are 126 and 116°, respectively, in FeL_2 and 92 and 145° in the cluster $FeCo_6Se_8(PEt_3)_4(PPh_2NTol)_2$ cluster counterpart.[16] The P−N bonds are slightly contracted in the ML_2 complexes compared with the cluster edge sites. This contraction is compensated for by an elongation of the Co−Se bonds in CoL_2, whereas in FeL_2, the contraction is offset by a lengthening of the Fe−N bonds. Solution magnetic moment determination using the Evans method[19] reveals that just like the cluster edge sites,[14−16] the ML_2 complexes feature high-spin M^{2+} metal centers. The magnetic moment is estimated to be 4.9(3) and 3.9(3) μ_B, respectively, for Fe and Co.

Adduct Formation. In solution, ML_2 complexes form adducts readily with exogenous ligands like pyridine-*N*-oxide (pyO) and *tert*-butyl isocyanide (CN^tBu). Single-crystal X-ray diffraction studies reveal that a single pyridine-*N*-oxide binds associatively and gives rise to five-coordinate monoadducts. In the solid state, the ML_2(Opy) adducts are isostructural and feature a distorted square-pyramidal geometry, with the exogenous ligand bound apically (Figure 3). In contrast, when binding to the cluster edge sites, monodentate exogenous ligands displace a selenium site, the metal preserving a four-coordinate, pseudotetrahedral geometry.[14,15] Although both M−Se bonding interactions are retained in the monometallic adduct ML_2(Opy), ligand coordination weakens them. The M−Se bonds elongate from 2.49 to 2.69 avg Å for Co and from 2.50 to 2.69 avg Å for Fe (Figure 3; Table S1) upon pyO binding. Binding constant determination using ^{1}H NMR spectroscopy reveals that pyO binds much more strongly to Fe than Co (10,826 vs 70 M^{-1}; Sections S2.3a and S2.3c). Nevertheless, the $ML_2(Opy)_x$ ($x < 1$) adducts are substoichiometric upon isolation in bulk, indicating the reversible binding of pyO to the metal center.

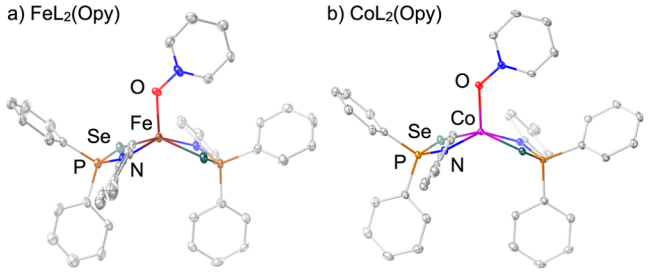

Figure 3. Solid-state structures of (a) FeL_2(Opy) and (b) CoL_2(Opy) adducts. Ellipsoids plotted at 50% probability. Hydrogen atoms are omitted for clarity.

While adding excess pyO to ML_2 complexes does not lead to bis-adduct formation, in situ NMR and IR spectroscopy analysis reveals that the stronger σ-donor and sterically less encumbered *tert*-butyl isocyanide might. For example, ^{1}H, ^{31}P, and ^{77}Se NMR spectroscopies suggest that a mixture of $FeL_2(CN^tBu)_2$ bis-adduct isomers forms when CN^tBu (minimum 2 equiv; Figures S6−S8) is added to the parent complex. The NMR analysis is particularly revealing for iron adduct formation since the putative $FeL_2(CN^tBu)_2$ isomers are diamagnetic, as expected for low-spin, hexacoordinate d^6 metal centers. The cobalt adducts display broad, paramagnetic ^{1}H NMR signals and no observable ^{31}P and ^{77}Se NMR peaks (Figure S12). In contrast to iron, the cobalt reaction mixture continues to evolve as increasing amounts of ligand are added (1−25 equiv of CN^tBu, Figure S12). This suggests that isocyanide binding is relatively weak, as also seen for pyridine-*N*-oxide. The vibrational spectrum of the $ML_2(CN^tBu)_x$ adducts contains two main features in the 2200−2125 cm^{-1} region, which could result from different ratios of *trans*- and *cis*-isocyanide isomers between the two metal complexes (Figures S5 and S11).

Reactivity with Oxygen Atom Transfer (OAT) Reagents. Although stable at room temperature for extended periods of time, thermolysis of the ML_2(Opy) monoadducts uncovers their differentiated reactivity. While the cobalt adduct CoL_2(Opy) is stable under thermolytic (12 h at 60 °C) or photolytic (3 h) conditions, FeL_2(Opy) converts to a mixture of partly oxidized products upon heating (1 h at 60 °C): a bimetallic mixed ligand complex $[FeLL']_n$, in which the Fe is bound by one amidophosphine selenide ligand (L) and one amidophosphine oxide ligand (L′ = $OPPh_2NTol$), and a bimetallic μ_2-oxo complex $[FeL_2]_2(\mu_2\text{-O})$ (Scheme 2a). The mixed ligand complex $[FeLL']_n$ is obtained pure using mesityl nitrile oxide (MesCNO), as discussed below (Scheme 2b).

In the solid state, $[FeL_2]_2(\mu_2\text{-O})$ features reveal two square-pyramidal, inequivalent FeL_2 centers (τ^5 = 0.08 and 0.19) bridged by a single oxo atom (Figure 4c). $[FeL_2]_2(\mu_2\text{-O})$ has a perfectly linear Fe−O−Fe angle (180.0°), and the Fe−O interatomic distances in $[FeL_2]_2(\mu_2\text{-O})$ are asymmetric (1.771(5) and 1.755(5) Å), which is not unusual for the Fe−O−Fe moiety.[20] The FeL_2 fragments in $[FeL_2]_2(\mu_2\text{-O})$ exhibit structural features similar to FeL_2(Opy), with elongated Fe−Se interatomic distances compared to the parent FeL_2 complex (2.50 vs 2.64 avg Å; Table S1). The magnetic moment of $[FeL_2]_2(\mu_2\text{-O})$, estimated using the Evans method to be 1.0(3) μ_B, is characteristic of two antiferromagnetically coupled Fe(III) S = 5/2 centers.[20,21] A feature at 350 (ε = 3,794 M^{-1} cm^{-1}) is observed in the electronic absorption spectrum and can be attributed to an oxo-to-Fe charge transfer transition (Figure S19).[22] Comparison of the infrared spectra of FeL_2 and $[FeL_2]_2(\mu_2\text{-O})$ enables the identification of a new feature at 852 cm^{-1}, which is attributed to the Fe−O−Fe asymmetric stretch (Figure S17).[20] Since the first synthetic diiron μ_2-oxo complex in 1933,[23] many synthetic reports of this

https://doi.org/10.1021/acs.organomet.4c00468
Organometallics 2025, 44, 335−339

Scheme 2. Reactivity with Oxygen Atom Donors

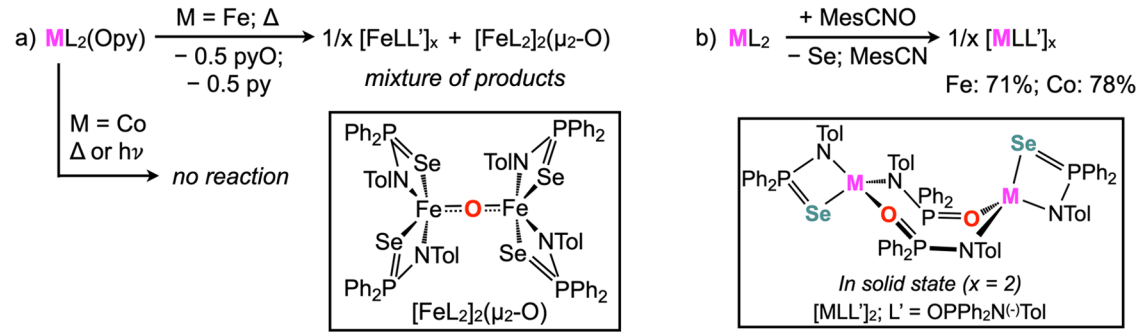

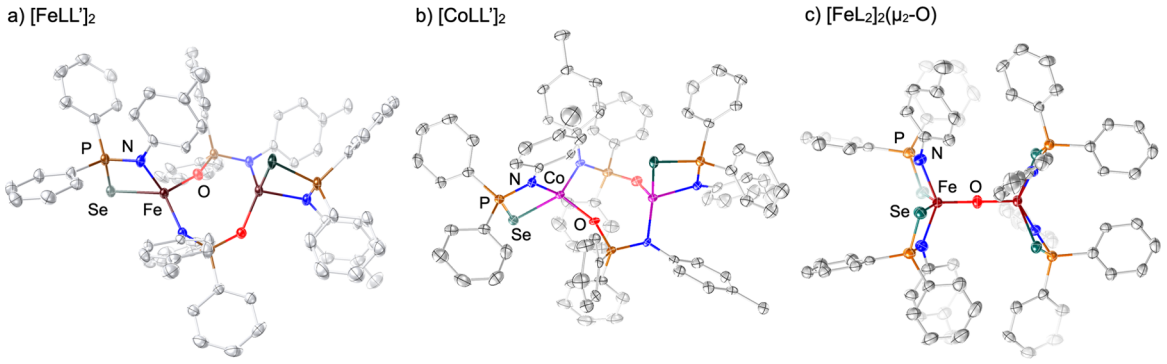

Figure 4. Solid-state structures for (a) $[FeLL']_2$, (b) $[CoLL']_2$, and (c) $[FeL_2]_2(\mu_2\text{-O})$. Ellipsoids plotted at 50% probability. Hydrogen atoms, disorder, and cocrystallized solvent molecules are omitted for clarity.

inorganic unit have emerged in platforms typically stabilized by O, N, or S chelating ligands.[20,21,24,25] $[FeL_2]_2(\mu_2\text{-O})$ represents the first structural report of an iron μ_2-oxo complex with Se in the primary coordination sphere.

Heating FeL_2 in the presence of excess pyO (3 equiv, 12 h, 60 °C) further advanced the oxidation process of the complex. Although not isolated in bulk, a single crystal of $[FeL'_2]_2(\mu_2\text{-O})$ was obtained from the complex reaction mixture and analyzed by X-ray diffraction (Section S4.8). Featuring a geometric structure similar to bicyclo[3.3.1]nonane, $[FeL'_2]_2(\mu_2\text{-O})$ is a bimetallic μ_2-oxo complex in which all the Se atoms have been replaced by oxygen atoms (Figure S28).

Although pyridine-*N*-oxide forms adducts readily with both the iron and cobalt ML_2 complexes, it oxidizes only the former. Our studies revealed its promiscuity toward oxidizing both the amidophosphine selenide ligands and the metal center in FeL_2. To explore the oxidation of the cobalt complex and to test if selective ligand oxidation could be achieved in the ML_2 complexes, we turned to a different oxygen transfer reagent. MesCNO is a stronger oxygen atom transfer reagent that is not prone to form stable adducts with metal complexes, but that can oxidize tertiary phosphines rapidly under ambient conditions.[26,27] Here, we discover that, unlike pyO, MesCNO reacts selectively with both FeL_2 and CoL_2 to produce the mixed ligand $[MLL']_n$ complexes quantitatively, without transferring an oxygen atom to the metal center (i.e., Fe).

Treatment of FeL_2 with MesCNO results in a color change from yellow to dark red and the quantitative formation of a soluble paramagnetic species identified as the mixed ligated complex $[FeLL']_n$ and a red precipitate (Scheme 2a). The insoluble byproduct is identified as red Se (1 equiv): the material is insoluble in common organic solvents, converts to a gray powder upon heating (i.e., gray Se),[28] and reacts with triphenylphosphine to produce $SePPh_3$ (Section S2.4). Single-crystal X-ray diffraction analysis confirmed the identity of the paramagnetic species to be the dimeric species $[FeLL']_2$ (Figure 4a). In the solid state, the amidophosphine oxide ligand chelates between two Fe centers to form an eight-membered ring (Fe−N−P−O−Fe−N−P−O) in a boat-chair conformation. Similarly, treating CoL_2 with stoichiometric amounts of MesCNO results in an immediate color change from green to blue and the quantitative formation of the mixed ligand complex $[CoLL']_2$. Single-crystal X-ray diffraction analysis of this species reveals that the cobalt mixed ligand complex is dimeric in the solid state and isostructural to the iron congener (Figure 4b).

CONCLUSIONS

The bis(amidophosphine selenide) coordination environment provides rich structural versatility, enabling the coordination of exogeneous ligands and the formation of bimetallic complexes. While the iron complex FeL_2 is more prone to oxidation than its Co counterpart, both complexes are susceptible to oxidation of the P═Se unit in the presence of oxygen atom transfer reagents. Although the reactivity of the analogous cluster-supported edge sites with oxygen atom donors has not been explored, we hypothesize that the Co_6Se_8 core may offer increased protection against ligand degradation compared to the ML_2 complexes.

ASSOCIATED CONTENT

Supporting Information

The Supporting Information is available free of charge at https://pubs.acs.org/doi/10.1021/acs.organomet.4c00468.

https://doi.org/10.1021/acs.organomet.4c00468
Organometallics 2025, 44, 335−339

General experimental considerations, synthetic protocols, and experimental characterization including crystallographic data (PDF)

Accession Codes

Deposition Numbers 2298461−2298464, 2298467, 2400818, 2400838, and 2400839 contain the supplementary crystallographic data for this paper. These data can be obtained free of charge via the joint Cambridge Crystallographic Data Centre (CCDC) and Fachinformationszentrum Karlsruhe Access Structures service.

AUTHOR INFORMATION

Corresponding Authors

Benjamin S. Mitchell − *Department of Chemistry, University of Washington, Seattle, Washington 98195, United States;* orcid.org/0000-0001-6585-2237; Email: bmitch1@uw.edu

Alexandra Velian − *Department of Chemistry, University of Washington, Seattle, Washington 98195, United States;* orcid.org/0000-0002-6782-7139; Email: avelian@uw.edu

Authors

Daniel Y. Zhou − *Department of Chemistry, University of Washington, Seattle, Washington 98195, United States*

Kelsey S. Zimmerman − *Department of Chemistry, University of Washington, Seattle, Washington 98195, United States*

Paige M. Gannon − *Department of Chemistry, University of Washington, Seattle, Washington 98195, United States*

Sebastian M. Krajewski − *Department of Chemistry, University of Washington, Seattle, Washington 98195, United States;* orcid.org/0000-0002-9755-2375

Werner Kaminsky − *Department of Chemistry, University of Washington, Seattle, Washington 98195, United States;* orcid.org/0000-0002-9100-4909

Complete contact information is available at: https://pubs.acs.org/10.1021/acs.organomet.4c00468

Notes

The authors declare no competing financial interest.

ACKNOWLEDGMENTS

This work was supported by the National Science Foundation (NSF) through a Faculty Early Career Development Program Award (1944843) and by the Research Corporation for Science Advancement through a Cottrell Scholars Award.

REFERENCES

(1) Fuchs, M.; Kuchen, W.; Peters, W. Übergangsmetallkomplexe [Et2P(S)NR]M/n, Vierringchelate mit Thiophosphinsäure-Organylamidato-Liganden [1]. *Z. Für Anorg. Allg. Chem.* **1987**, *545* (2), 75−82.

(2) Deeg, A.; Kuchen, W.; Langsch, D.; Mootz, D.; Peters, W.; Wunderlich, H. Nickel(II)- und Cobalt(II)-Thiophosphinsäure-N-Organylamidato-Chelate [R2P(S)NR′]2M: Magnetische Eigenschaften und Kristallstrukturen. *Z. Für Anorg. Allg. Chem.* **1991**, *606* (1), 119−132.

(3) Song, X.; Bochmann, M. Synthesis of Phosphinochalcogenoic Amidato Complexes of Divalenttransition Metals and Their Thermolysis to Metal Selenide and Telluridephases. *J. Chem. Soc., Dalton Trans.* **1997**, *15*, 2689−2692.

(4) Bochmann, M.; Bwembya, G. C.; Hursthouse, M. B.; Coles, S. J. Synthesis of Phosphinochalcogenoic Amidato Complexes of Zinc and Cadmium. The Crystal and Molecular Structure of [Zn{But2P(Se)-NPri}2]. *J. Chem. Soc., Dalton Trans.* **1995**, *17*, 2813−2817.

(5) Kim, Y. K.; Livinghouse, T.; Horino, Y. Chelating Bis(Thiophosphinic Amidate)s as Versatile Supporting Ligands for the Group 3 Metals. An Application to the Synthesis of Highly Active Catalysts for Intramolecular Alkene Hydroamination. *J. Am. Chem. Soc.* **2003**, *125* (32), 9560−9561.

(6) Bhattacharjee, J.; Das, S.; Kottalanka, R. K.; Panda, T. K. Hydroamination of Carbodiimides, Isocyanates, and Isothiocyanates by a Bis(Phosphinoselenoic Amide) Supported Titanium(IV) Complex. *Dalton Trans.* **2016**, *45* (44), 17824−17832.

(7) Bhattacharjee, J.; Harinath, A.; Banerjee, I.; Nayek, H. P.; Panda, T. K. Highly Active Dinuclear Titanium(IV) Complexes for the Catalytic Formation of a Carbon−Heteroatom Bond. *Inorg. Chem.* **2018**, *57* (20), 12610−12623.

(8) Platel, R. H.; Hodgson, L. M.; White, A. J. P.; Williams, C. K. Synthesis and Characterization of a Series of Bis(Oxo/Thiophosphinic)Diamido Yttrium Complexes and Their Application as Initiators for Lactide Ring-Opening Polymerization. *Organometallics* **2007**, *26* (20), 4955−4963.

(9) Harinath, A.; Bhattacharjee, J.; Sarkar, A.; Nayek, H. P.; Panda, T. K. Ring Opening Polymerization and Copolymerization of Cyclic Esters Catalyzed by Group 2 Metal Complexes Supported by Functionalized P−N Ligands. *Inorg. Chem.* **2018**, *57* (5), 2503−2516.

(10) Faller, J. W.; Friss, T.; Parr, J. Hemilability and Regioselectivity in Palladium and Platinum Complexes of Dppm(*E*) [*E* = O, S, Se] Ligands. *J. Organomet. Chem.* **2010**, *695* (24), 2644−2650.

(11) Stec, W. J.; Okruszek, A.; Michalski, J. Organophosphorus Compounds of Sulfur and Selenium. Stereochemistry of Oxidation of Thiono- and Selenophosphoryl Compounds with Hydrogen Peroxide. *J. Org. Chem.* **1976**, *41* (2), 233−238.

(12) Stec, W. J.; Okruszek, A.; Lesiak, K.; Uznanski, B.; Michalski, J. New Synthesis of S(Se)-Alkyl Phosphorothio(Seleno)Lates from the Corresponding Phosphoroanilidates. Stereospecific Cleavage of the Phosphorus-Nitrogen Bond in Chiral Phosphoroanilidates. *J. Org. Chem.* **1976**, *41* (2), 227−233.

(13) Arnone, A.; Pregnolato, M.; Resnati, G.; Terreni, M. Conversion of Thio- and Selenophosphoryl into Phosphoryl Group by Perfluoro Cis-2,3-Dialkyloxaziridines. *J. Org. Chem.* **1997**, *62* (18), 6401−6403.

(14) Kephart, J. A.; Mitchell, B. S.; Chirila, A.; Anderton, K. J.; Rogers, D.; Kaminsky, W.; Velian, A. Atomically Defined Nanopropeller $Fe_3Co_6Se_8(Ph_2PNTol)_6$: Functional Model for the Electronic Metal−Support Interaction Effect and High Catalytic Activity for Carbodiimide Formation. *J. Am. Chem. Soc.* **2019**, *141* (50), 19605−19610.

(15) Kephart, J. A.; Romero, C. G.; Tseng, C.-C.; Anderton, K. J.; Yankowitz, M.; Kaminsky, W.; Velian, A. Hierarchical Nanosheets Built from Superatomic Clusters: Properties, Exfoliation and Single-Crystal-to-Single-Crystal Intercalation. *Chem. Sci.* **2020**, *11* (39), 10744−10751.

(16) Mitchell, B. S.; Chirila, A.; Kephart, J. A.; Boggiano, A. C.; Krajewski, S. M.; Rogers, D.; Kaminsky, W.; Velian, A. Metal−Support Interactions in Molecular Single-Site Cluster Catalysts. *J. Am. Chem. Soc.* **2022**, *144* (40), 18459−18469.

(17) Kephart, J. A.; Mitchell, B. S.; Kaminsky, W.; Velian, A. Multi-Active Site Dynamics on a Molecular Cr/Co/Se Cluster Catalyst. *J. Am. Chem. Soc.* **2022**, *144* (21), 9206−9211.

(18) Mitchell, B. S.; Krajewski, S. M.; Kephart, J. A.; Rogers, D.; Kaminsky, W.; Velian, A. Redox-Switchable Allosteric Effects in Molecular Clusters. *JACS Au* **2022**, *2* (1), 92−96.

(19) Evans, D. F. The Determination of the Paramagnetic Susceptibility of Substances in Solution by Nuclear Magnetic Resonance. *J. Chem. Soc.* **1959**, *0*, 2003−2005.

(20) Kurtz, D. M., Jr. Oxo- and Hydroxo-Bridged Diiron Complexes: A Chemical Perspective on a Biological Unit. *Chem. Rev.* **1990**, *90* (4), 585−606.

(21) Murray, K. S. Binuclear Oxo-Bridged Iron(iii) Complexes. *Coord. Chem. Rev.* **1974**, *12* (1), 1−35.

(22) Reem, R. C.; McCormick, J. M.; Richardson, D. E.; Devlin, F. J.; Stephens, P. J.; Musselman, R. L.; Solomon, E. I. Spectroscopic Studies of the Coupled Binuclear Ferric Active Site in Methemerythrins and Oxyhemerythrin: The Electronic Structure of Each Iron Center and the Iron-Oxo and Iron-Peroxide Bonds. *J. Am. Chem. Soc.* **1989**, *111* (13), 4688−4704.
(23) Pfeiffer, P.; Breith, E.; Lübbe, E.; Tsumaki, T. Tricyclische Orthokondensierte Nebenvalenzringe. *Justus Liebigs Ann. Chem.* **1933**, *503* (1), 84−130.
(24) Guchhait, T.; Sasmal, S.; Khan, F. S. T.; Rath, S. P. Oxo- and Hydroxo-Bridged Diiron(III) Porphyrin Dimers: Inorganic and Bio-Inorganic Perspectives and Effects of Intermacrocyclic Interactions. *Coord. Chem. Rev.* **2017**, *337*, 112−144.
(25) Sorokin, A. B. Recent Progress on Exploring M-Oxo Bridged Binuclear Porphyrinoid Complexes in Catalysis and Material Science. *Coord. Chem. Rev.* **2019**, *389*, 141−160.
(26) Cai, X.; Majumdar, S.; Fortman, G. C.; Frutos, L. M.; Temprado, M.; Clough, C. R.; Cummins, C. C.; Germain, M. E.; Palluccio, T.; Rybak-Akimova, E. V.; Captain, B.; Hoff, C. D. Thermodynamic, Kinetic, and Mechanistic Study of Oxygen Atom Transfer from Mesityl Nitrile Oxide to Phosphines and to a Terminal Metal Phosphido Complex. *Inorg. Chem.* **2011**, *50* (19), 9620−9630.
(27) Palluccio, T. D.; Rybak-Akimova, E. V.; Majumdar, S.; Cai, X.; Chui, M.; Temprado, M.; Silvia, J. S.; Cozzolino, A. F.; Tofan, D.; Velian, A.; Cummins, C. C.; Captain, B.; Hoff, C. D. Thermodynamic and Kinetic Study of Cleavage of the N−O Bond of N-Oxides by a Vanadium(III) Complex: Enhanced Oxygen Atom Transfer Reaction Rates for Adducts of Nitrous Oxide and Mesityl Nitrile Oxide. *J. Am. Chem. Soc.* **2013**, *135* (30), 11357−11372.
(28) Mills, K.C. *Thermodynamic Data for Inorganic Sulphides, Selenides and Tellurides*; Butterworths: London, 1974.

https://doi.org/10.1021/acs.organomet.4c00468
Organometallics 2025, 44, 335−339